Appendix 1:

Ballast Water Modelling

Ballast Water Dispersal Modelling

Steensby Inlet, Nunavut

Report Prepared

for

Baffinland Iron Mines Corporation

by

Coastal and Ocean Resources Inc.

Victoria, BC

and

International Tsunami Research Inc.

Sidney, BC

December 13, 2011

Introduction

Coastal and Ocean Resources Inc. was asked to undertake a preliminary estimation of the redistribution and dispersal of ballast water discharged from iron ore bulk carriers at the proposed port site in Steensby Inlet. This initial analysis is to provide an indication of the probable dispersion pathways and resulting concentrations of ballast water throughout the inlet under the influence of tidal, estuarine and wind-driven circulation. The dispersal modelling is based on time-varying, three-dimensional circulation in Steensby Inlet derived using the advanced Regional Ocean Modeling System (ROMS).

The basic scenarios provided for the modelling are:

- ballast water originates in the central North Atlantic
- 200,000 m^3 of ballast water are discharged twice a week at the dock during ice-covered conditions in the inlet
- 70,000 m^3 of ballast water are discharged twice a week at the dock during open water conditions
- there are 104 visits of vessels discharging ballast water per year (i.e., two visits per week)
- modelling is to show the cumulative effects in the basin after one year of discharge at the port.

A sensitivity analysis was also performed wherein: (1) twice as much ballast water was discharged during both ice-covered and open-water conditions (i.e., 200,000 m^3 four times per week when ice is present; 70,000 m^3 four times per week during open water conditions); and, (2) half as much ballast water is discharged (i.e., 200,000 m^3 once per week when ice is present; 70,000 m^3 once per week during open water conditions).

The results of the modelling and analysis show the contribution of ballast water to the water column at different depths in the basin after one year of discharging water at the port area.

Several assumptions were necessary in this initial assessment:

- Ballast water from the North Atlantic during winter had a temperature of 6^o C and a salinity of 35.0 psu (practical salinity units); in actuality, ballast water would be taken on over a considerable segment of the ship track in the North Atlantic and, because of a strong east-west gradient in salinity and temperature, it would be a mixture of waters with varying temperature and salinity (and hence, density) properties.

- This initial coarse-grid model (400 m × 400 m) did not permit an assessment of density flows of ballast water. A nested fine-grid model (50 m × 50 m) would allow processes such as density flows at the input location to be considered.

- Ballast water physical properties (specifically temperature) are assumed to remain constant between the zone where the ballast water is taken on by the vessel until it is discharged at the port; in reality, ballast water temperature will likely change as a result of cooling from ambient seawater along the route, and, possibly, a slight warming due to treatment processes. The effects of these processes could not be ascertained because of uncertainty with respect to the vessel design and ballast treatment processes planned.

- It is assumed that ballast water is to be discharged from a single point (within a single model grid cell), near the ocean surface, at the port site; in actuality, there may be several discharge points and varying rates of discharge depending on the vessel design and load planning. None of these details is presently available.

- Two distinct oceanic conditions were modelled: ice-covered ocean and ice-free ocean. At this point, physical processes during freeze-up and ice break-up are not incorporated in the model and are outside the timeframe for this assessment. Incorporation of some of these processes could be investigated following further refinements to the model.

A more refined assessment, using a fine-grid model (50 m resolution) for the port area nested within the coarse-grid model for Steensby Inlet, could be carried out to determine better the precise long-term dispersion and concentrations of ballast water in the basin. As the vessel design and operations become better defined these details could eventually be incorporated into the model.

Methodology

The model used for circulation in Steensby Inlet is the Regional Ocean Model System (ROMS); complete details of the model are beyond the scope of this report but can be found at http://www.myroms.org/ . ROMS is a state-of-the-art, three-dimensional, time-stepping numerical model system which has only recently become available for use outside the academic community. This free-surface, terrain-following, primitive equation numerical simulation model has been widely used by the scientific community for a diverse range of applications, with specific focus on coastal regions of the World Ocean. In the present application, it is able to simulate the effects of tidally driven currents (the primary source of kinetic energy in the Steensby Inlet basin) with wind-driven currents and the surface-enhanced estuarine flow resulting from fresh water runoff. Because the present ROMS model does not have the capability to accommodate under-ice frictional effects on currents, modifications to the standard parameterization of frictional effects had to be introduced to better model circulation during ice-covered periods (St-Laurent *et al*. 2008). The model does allow for the delivery of waters from a point source and for the timing of this delivery

to be specified; it was this feature which was invoked to model the input of ballast water into the circulation regime at the Steensby proposed port site.

All bathymetric data available for Steensby Inlet were used to define the basin morphology for the model (Figure 1). Aside from a very small volume of data collected by the Canadian Hydrographic Service in central and southern Steensby Inlet, the only bathymetric data for the region is that acquired by various survey companies during the course of environmental and engineering investigations for Baffinland Iron Mines Corp. These data were concentrated along the proposed shipping route to the proposed port site, in shallow-water areas near the port site and in central Steensby Inlet. A few widely spaced, reconnaissance survey lines were also collected across the basin in anticipation of their need in constructing a regional ocean circulation model. Water depths in northern Steensby Inlet are generally very shallow, and marked by a complex morphology of shoals and small basins; the survey vessel carrying out the reconnaissance survey lines was unable to work in these areas because of the unknown water depths and, as a result, this is the most poorly known part of the Steensby Inlet basin. Vertical aerial photo imagery collected during a polar bear survey was used to confirm the shallow portions of this area in Steensby Inlet. A 50 m x 50 m bathymetric grid was created from the available data; where data were absent, Kriging methodology was used to interpolate grid values from points of known data.

Because the standard (full) version of the ROMS was not designed for the full coupled dynamics and thermodynamics of the ocean-sea-ice interaction, and existing coupled models have been developed for basin-scale application, we restricted our modelling to the specific cases of "ice-free" and "ice-covered" conditions. These two conditions were provided by the basin-scale model developed by the Institut des Science de la Mer (ISMER) at the Université du Québec à Rimouski and Fisheries and Oceans Canada (Saucer et al., 2004).

The ISMER model is a realistic primitive equation, z-coordinate, 3D ocean circulation model coupled to the dynamics and thermodynamics of the two-layer sea-ice model and one-layer snow cover. The combined model was forced by atmospheric fluxes provided by analysis of the Canadian weather forecasting model, and tidal forcing through the lateral open boundaries. The model provides realistic seasonal cycling of the entire basin, as well as major tides, and wind-induced and density-related ocean currents. The horizontal resolution of the ISMER model is 10 km and the vertical resolution is 10 m, which is adequate to resolve the main features of the basin-scale circulation, but too coarse to account for the precise details of inlet-scale circulation.

In the current application we used results of the ISMER Foxe Basin modelling to set up the initial stratification and lateral boundary conditions for tracers during both ice-covered and ice-free periods. As well, we used CTD profiles in Steensby Inlet to set-up the initial and boundary conditions.

Also, we used results of the sea surface height variability of the ISMER modelling to calculate the tidal constituents at the Steensby Inlet open boundary for both the ice-covered and ice-free periods. These constituents were then used in the present ROMS Steensby Inlet tidal modelling.

In our model, the atmospheric forcing is limited by wind effects during ice-free conditions, with wind data collected over a two-year period near the port area (RWDI 2008), and from NOAA's NCEP/NCAR North American Regional Reanalysis project (http://www.emc.ncep.noaa.gov/mmb/rreanl/). Hourly-averaged wind data from the meteorological station span the period from September 2006 to September 2008 (with some gaps); three-hourly reanalysis wind data cover a much longer period of 2005-2010.

Freshwater input from four sources around the perimeter of the basin (Table 1; Figure 1) was used to drive the estuarine circulation in the basin (Knight-Piésold Ltd. 2011).

The location of the ballast water discharge at the proposed port site (Site 5) is shown in Figure 1. Details of the bathymetry in central Steensby Inlet near the proposed port are shown in Figure 2. Figure 2 also defines the three transects of ballast water concentration presented later in this analysis.

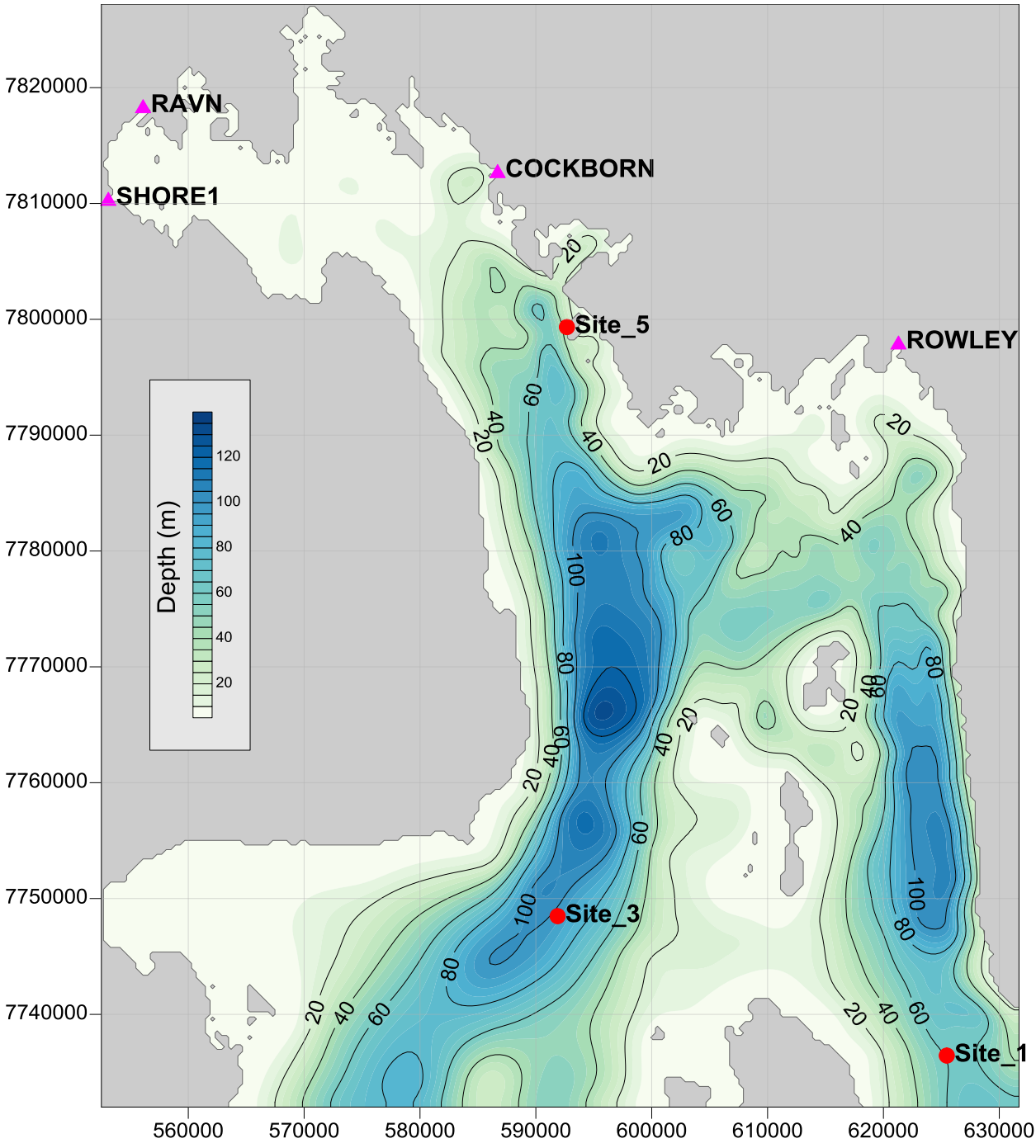

Figure 1. Modelled area of Steensby Inlet showing the location of freshwater sources (pink triangles), current meter and tide gauge sites (red circles) and the port site (Site 5).

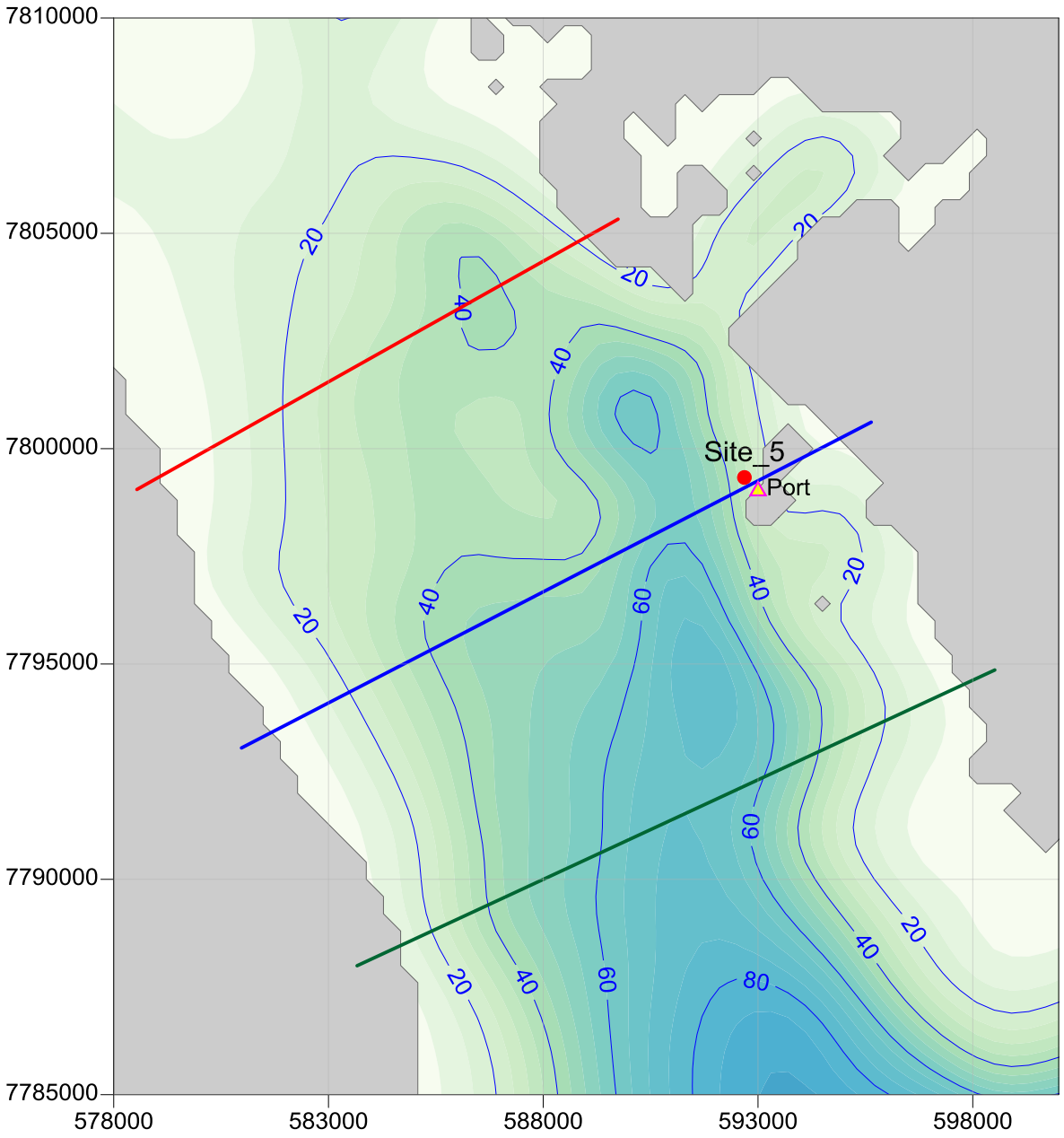

Figure 2. The central zone in Steensby Inlet near the proposed port showing the location of Site 5, the source of ballast water discharge (port), and cross-sections (red, blue and green lines) where ballast water concentration is displayed (see below).

Table 1. Major freshwater sources in Steensby Inlet with gauging data for 2008. (Knight-Piésold Ltd., 2011)

	Drainage Area (km^2)	Outlet Location at Steensby Inlet	
Cockburn River:	**1,900**	**70°25'15"N**	**78°38'35"W**
Ravn River:	**14,450**	**70°27'40"N**	**79°29'15"W**
Rowley River:	**4,485**	**70°15'00"N**	**77°47'00"W**
Steensby Shore1:	**1,750**	**70°23'40"N**	**79°33'00"W**

The model was validated using time series records from tide gauges, bottom-pressure recorders, and Acoustic Doppler Current Profilers (ADCPs) installed near the port area and near the southern entrance to Steensby Inlet in 2007 and 2008 (ASL, 2008; AMEC 2009, see Figure 1). The comparison between observed and modelled tidal constituents (Tables 2-6, Figures 3 and 4) shows good agreement. Water property data spanning the entire water column were obtained using conductivity-temperature-depth (CTD) profilers at many sites in Steensby Inlet in 2007, 2008 and 2010. These data were examined during the model development and application and provided an important source for the initialisation of the model..

Table 2. Comparison between modelled and measured barotropic tidal current constituents at Site 1 (see Figure 1 for the location of the site).

	U		V		Ellipse				
	H, cm/s	G, degrees	H, cm/s	G, degrees	Major, cm/s	Minor, cm/s	Incl, degrees	Phase, degrees	
MSF	1.42	185.1	1.67	47.5	2.05	-0.78	128.8	30.4	
O1	1.11	24.0	2.42	215.1	2.66	-0.20	114.5	213.2	
P1	1.08	110.1	1.76	292.2	2.07	-0.03	121.6	291.6	
K1	3.28	110.1	5.32	292.2	6.25	-0.10	121.6	291.6	**ADCP**
N2	1.63	76.6	2.49	257.8	2.97	-0.03	123.2	257.4	
M2	10.40	121.8	17.22	296.2	20.10	0.86	121.1	297.7	
S2	3.35	179.3	6.35	356.6	7.18	0.14	117.8	357.2	
K2	0.91	179.3	1.73	356.6	1.95	0.04	117.8	357.2	
M4	2.65	24.2	3.68	197.0	4.53	0.27	125.7	199.5	
MS4	2.55	78.6	3.53	257.3	4.35	0.05	125.8	257.8	

	U		V		Ellipse				
	H, cm/s	G, degrees	H, cm/s	G, degrees	Major, cm/s	Minor, cm/s	Incl, degrees	Phase, degrees	
MSF	0.18	96.9	0.13	290.7	0.22	-0.03	143.3	281.8	
O1	0.85	14.4	2.21	205.7	2.36	-0.16	110.9	204.2	
P1	0.76	104.6	1.85	289.5	2.00	-0.06	112.3	288.8	
K1	2.34	112.1	5.46	295.6	5.94	-0.13	113.2	295.1	**MODEL**
N2	1.98	52.0	4.13	241.5	4.57	-0.30	115.4	239.8	
M2	10.35	99.8	23.77	288.6	25.88	-1.46	113.4	287.2	
S2	2.32	143.3	5.45	338.1	5.90	-0.55	112.6	335.9	
K2	0.94	192.7	2.09	17.9	2.29	-0.08	114.2	17.1	
M4	2.21	42.9	4.80	218.6	5.28	0.15	114.6	219.3	
MS4	1.71	91.0	3.89	269.3	4.25	0.05	113.8	269.5	

Table 3. Comparison between modelled and measured barotropic tidal current constituents at Site 3 (see Figure 1 for the location of the site).

	U		V		Ellipse				
	H, cm/s	G, degrees	H, cm/s	G, degrees	Major, cm/s	Minor, cm/s	Incl, degrees	Phase, degrees	
MSF	2.06	186.0	0.34	95.1	2.06	-0.34	179.8	6.1	
O1	0.40	337.7	0.80	288.3	0.85	-0.29	69.3	295.6	
P1	0.23	46.6	0.45	34.8	0.51	-0.04	63.4	37.2	
K1	0.70	46.6	1.37	34.8	1.53	-0.13	63.4	37.2	**ADCP**
N2	3.53	242.0	4.85	251.8	5.98	0.48	54.1	248.4	
M2	20.54	248.9	25.93	259.4	32.95	2.95	51.7	255.4	
S2	7.05	324.4	9.45	333.4	11.75	0.89	53.4	330.2	
K2	1.92	324.4	2.57	333.4	3.20	0.24	53.4	330.2	
M4	1.02	287.5	2.32	155.4	2.43	-0.72	107.9	149.9	
MS4	0.45	10.2	2.22	217.0	2.26	-0.20	100.3	216.0	

	U		V		Ellipse				
	H, cm/s	G, degrees	H, cm/s	G, degrees	Major, cm/s	Minor, cm/s	Incl, degrees	Phase, degrees	
MSF	0.22	357.6	0.39	122.5	0.41	0.17	111.5	131.6	
O1	0.17	338.9	0.39	350.5	0.43	0.03	66.7	348.7	
P1	0.41	120.4	0.66	133.6	0.77	0.08	58.3	129.9	
K1	0.74	96.6	1.23	112.9	1.43	0.18	59.4	108.6	**MODEL**
N2	2.83	240.8	4.20	243.4	5.06	0.11	56.0	242.6	
M2	16.09	250.4	24.68	258.3	29.41	1.84	57.0	256.0	
S2	4.36	315.9	6.38	322.5	7.72	0.41	55.8	320.4	
K2	1.44	352.9	2.28	359.6	2.69	0.14	57.7	357.7	
M4	2.17	177.9	3.38	185.6	4.01	0.25	57.4	183.4	
MS4	1.73	228.3	2.75	235.4	3.25	0.18	57.9	233.4	

Table 4. Comparison between modelled and measured barotropic tidal current constituents at Site 5 (see Figure 1 for the location of the site).

	U		V		Ellipse				
	H, cm/s	G, degrees	H, cm/s	G, degrees	Major, cm/s	Minor, cm/s	Incl, degrees	Phase, degrees	
MSF	0.22	246.6	0.98	238.1	1.01	-0.03	77.5	238.5	
O1	0.31	228.9	0.48	230.3	0.57	0.01	57.5	229.9	
P1	0.12	339.3	0.27	289.8	0.28	-0.09	71.6	295.8	
K1	0.37	339.3	0.82	289.8	0.86	-0.27	71.6	295.8	**ADCP**
N2	0.99	224.5	2.51	216.6	2.70	-0.13	68.5	217.7	
M2	4.26	248.4	11.84	240.1	12.57	-0.58	70.4	241.1	
S2	1.93	318.2	4.98	307.8	5.33	-0.33	69.0	309.2	
K2	0.53	318.2	1.35	307.8	1.45	-0.09	69.0	309.2	
M4	1.53	184.8	2.26	189.7	2.73	0.11	55.8	188.1	
MS4	1.59	245.0	2.76	245.4	3.18	0.01	60.1	245.3	

	U		V		Ellipse				
	H, cm/s	G, degrees	H, cm/s	G, degrees	Major, cm/s	Minor, cm/s	Incl, degrees	Phase, degrees	
MSF	0.22	357.6	0.39	122.5	0.41	0.17	111.5	131.6	
O1	0.17	338.9	0.39	350.5	0.43	0.03	66.7	348.7	
P1	0.41	120.4	0.66	133.6	0.77	0.08	58.3	129.9	
K1	0.74	96.6	1.23	112.9	1.43	0.18	59.4	108.6	**MODEL**
N2	2.83	240.8	4.20	243.4	5.06	0.11	56.0	242.6	
M2	16.09	250.4	24.68	258.3	29.41	1.84	57.0	256.0	
S2	4.36	315.9	6.38	322.5	7.72	0.41	55.8	320.4	
K2	1.44	352.9	2.28	359.6	2.69	0.14	57.7	357.7	
M4	2.17	177.9	3.38	185.6	4.01	0.25	57.4	183.4	
MS4	1.73	228.3	2.75	235.4	3.25	0.18	57.9	233.4	

Table 5. Comparison between tidal constituents for the modelled and measured sea level in the ice-free period (model) and BPR-1050 (September).

	RBR -1050		MODEL	
	H ,cm	**G, degrees**	**H, cm**	**G, degrees**
O1	15.17	343.4	6.95	316. 7
P1	7.74	52.9	6.16	36.8
K1	23.39	52.9	13.24	54.0
N2	29.67	320.4	27.69	329.1
M2	142.17	352.8	142.57	355.6
S2	50.47	63.0	47.33	57.8
K2	13.73	63.0	5.86	47.8
M4	10.34	278.1	12.47	295.09
MS4	9.49	347.0	10.04	343.78

Table 6. Comparison between tidal constituents for the modelled and measured sea level in the ice-covered period (model) and BPR 1050 (January).

	RBR -1050		MODEL	
	H, cm	**G, degrees**	**H, cm**	**G, degrees**
O1	13.96	351.6	7.12	329.7
P1	6.36	46.0	4.11	47.2
K1	19.20	46.0	12.04	55.1
N2	23.02	328.1	27.72	326.0
M2	131.33	353.1	135.04	355.5
S2	50.58	61.1	41.46	54.1
K2	13.76	61.1	9.56	65.9
M4	6.57	255.5	12.50	283.7
MS4	4.52	346.7	8.35	343.0

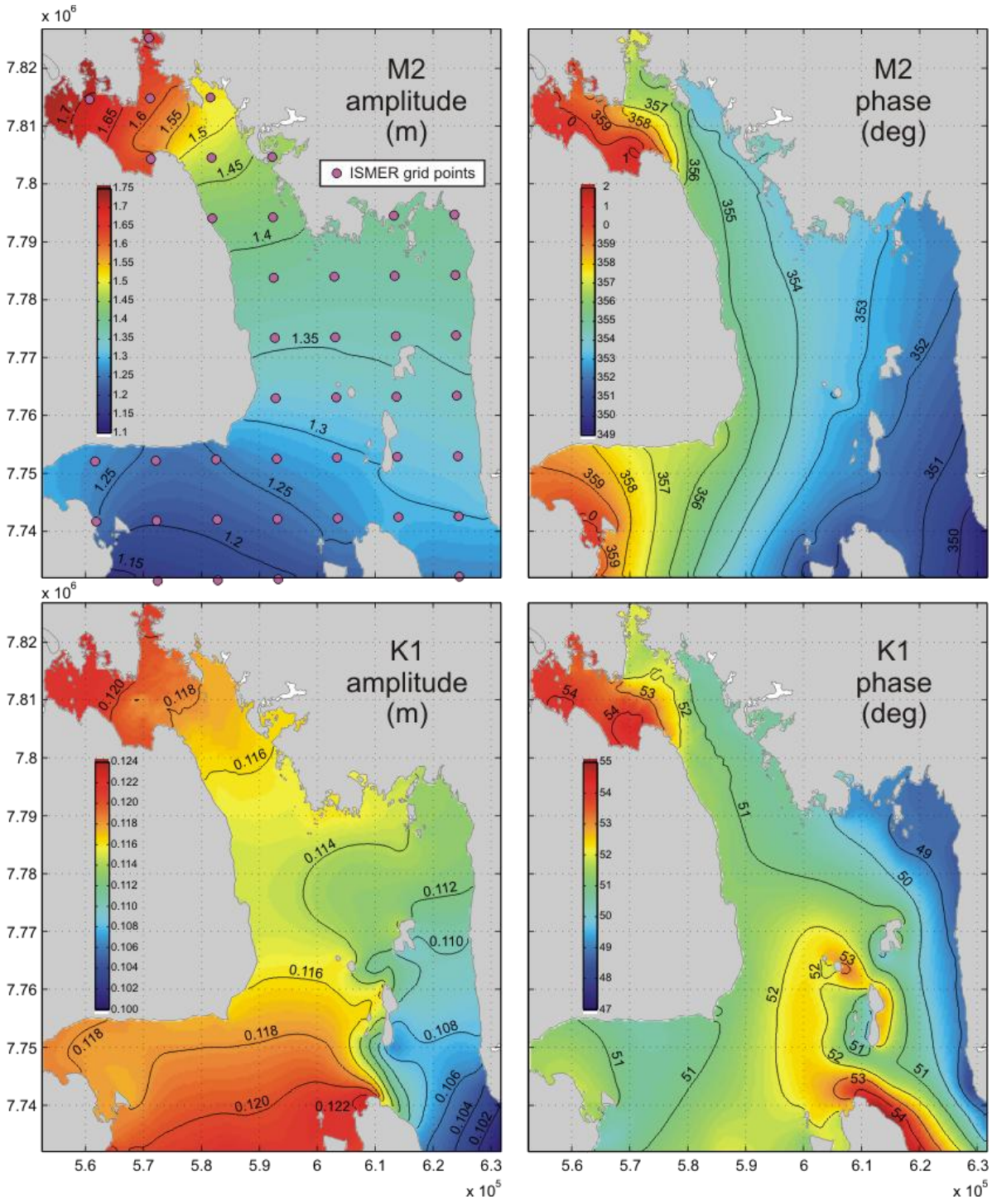

Figure 3. Modelled tidal constituents used in the ROMS circulation model for Steensby Inlet. Model results were validated using the tide gauge and pressure sensor data from the port area and the southern entrance to Steensby Inlet (Figure 1). ISMER grid points refer to the general model developed by the Institut des Science de la Mer at the Université du Québec à Rimouski and Fisheries and Oceans Canada (Saucier et al., 2004).

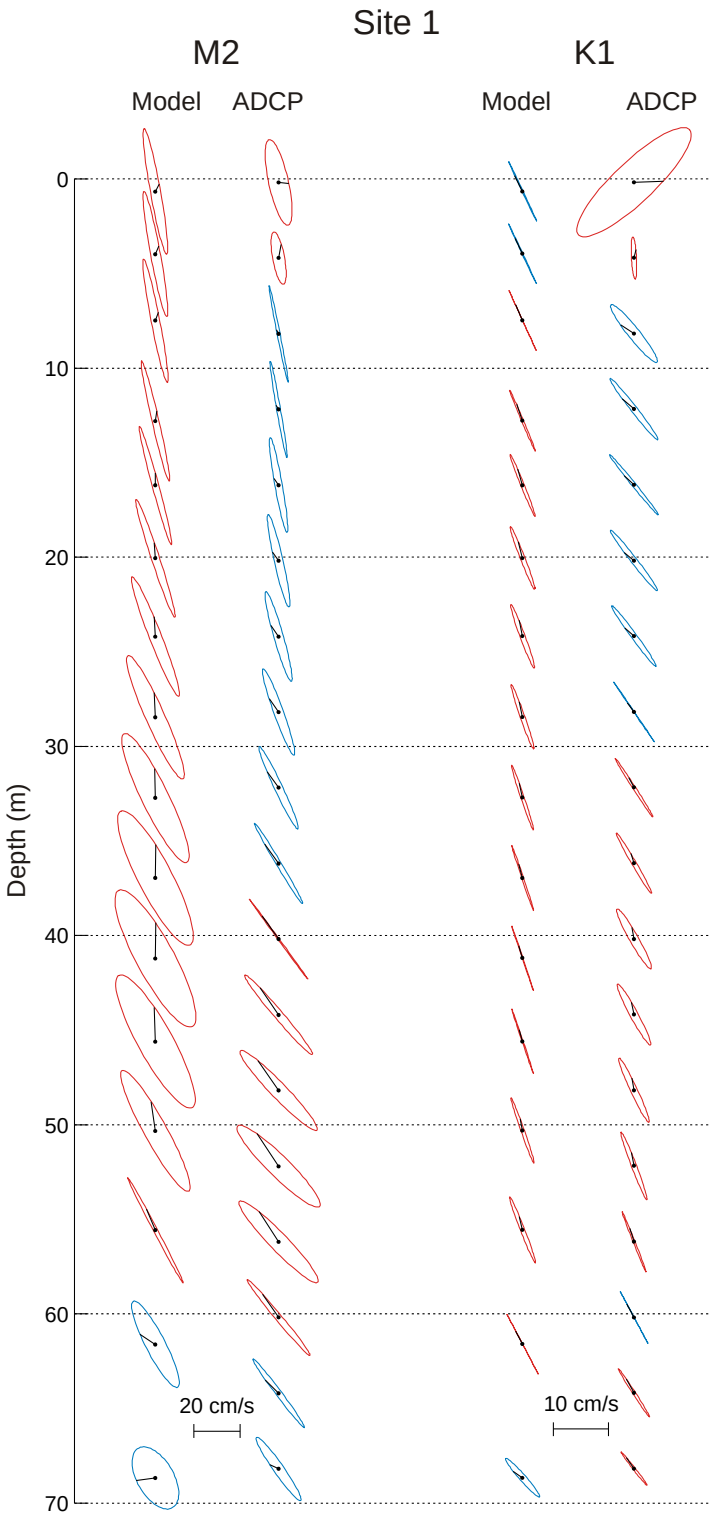

Figure 4a. Comparison between tidal ellipses for the M2 and K1 tidal constituents at Site 1 (see Figure 1 for the location of the site). Blue ellipses correspond to the counter-clockwise rotation of the tidal vector, and red corresponds to the clockwise rotation.

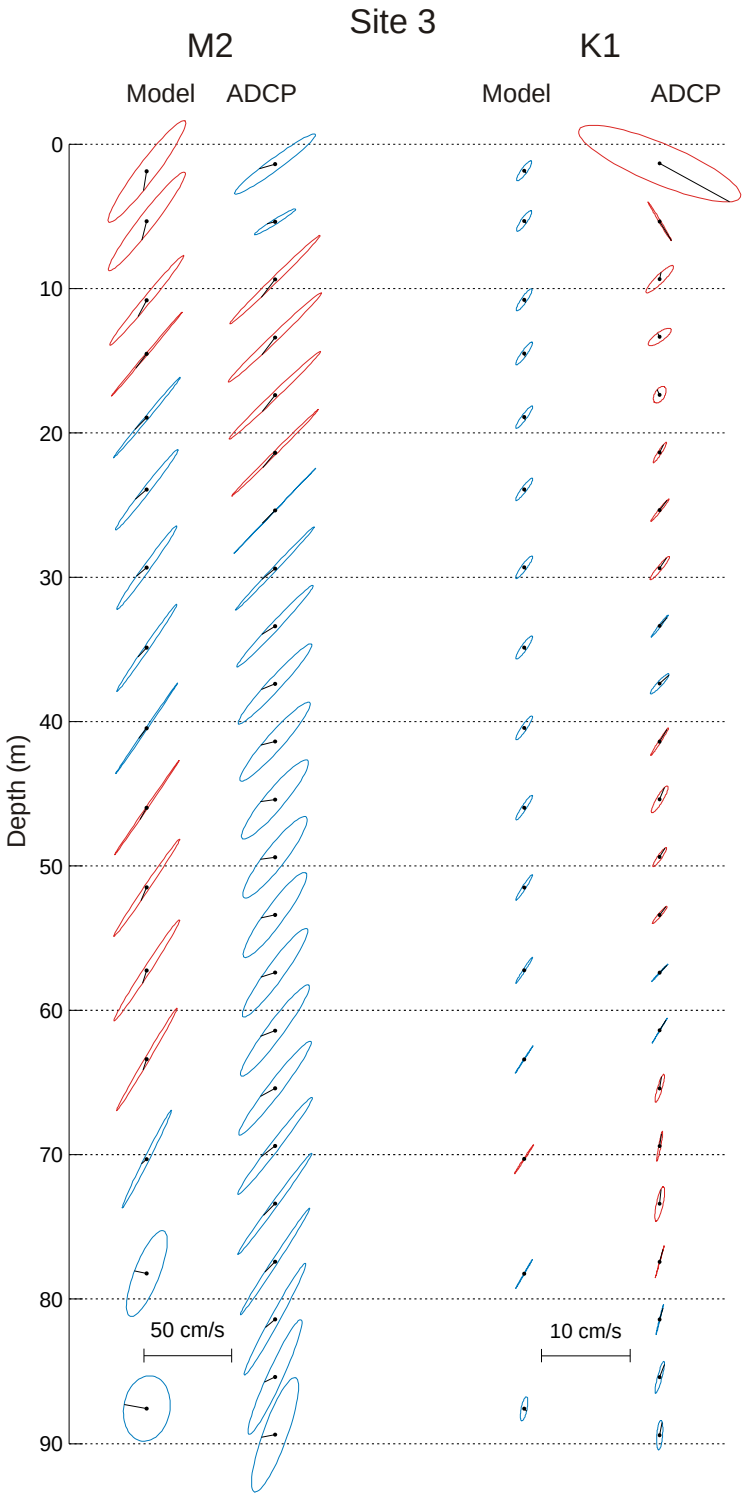

Figure 4b. Comparison between tidal ellipses for the M2 and K1 tidal constituents at Site 3 (see Figure 1 for the location of the site). Blue ellipses correspond to the counter-clockwise rotation of the tidal vector, and red corresponds to the clockwise rotation.

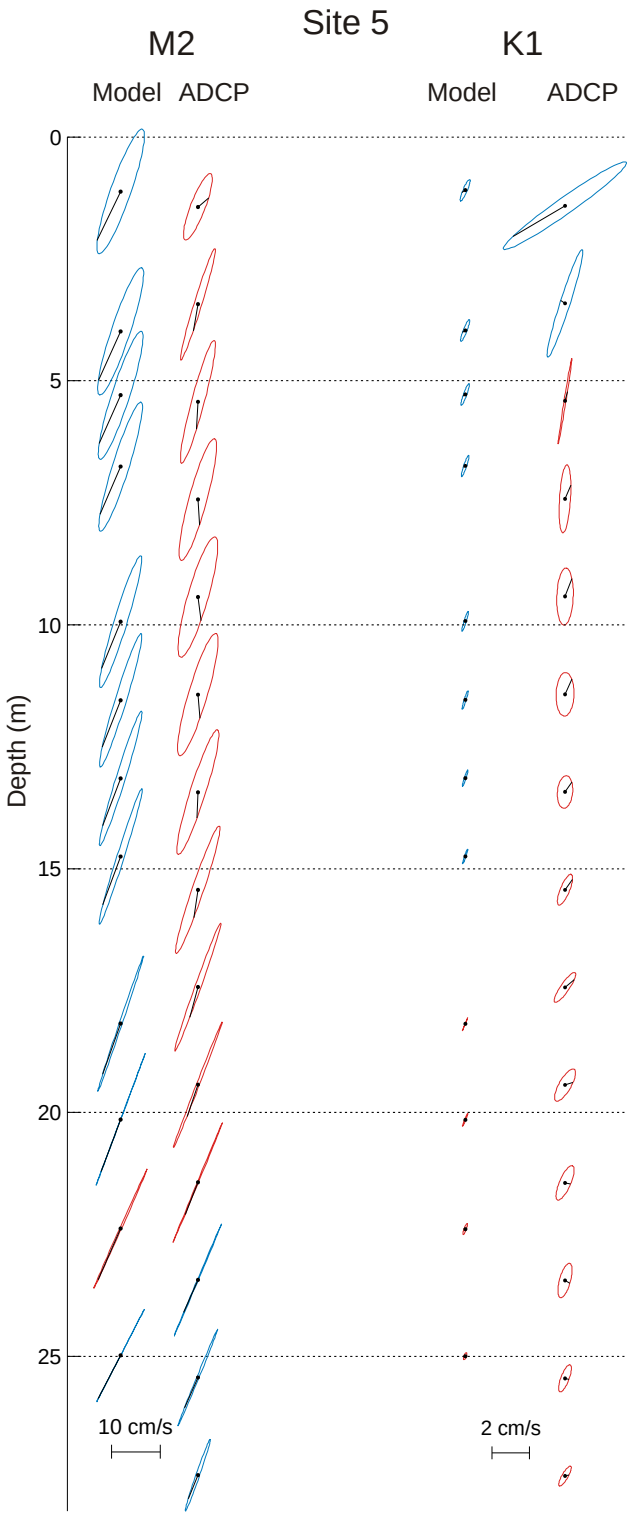

Figure 4c. Comparison between tidal ellipses for the M2 and K1 tidal constituents at Site 5 (see Figure 1 for the location of the site). Blue ellipses correspond to the counter-clockwise rotation of the tidal vector, and red corresponds to the clockwise rotation.

Results

The results of the ballast water modelling under the baseline conditions are shown in Figures 5 through 10.

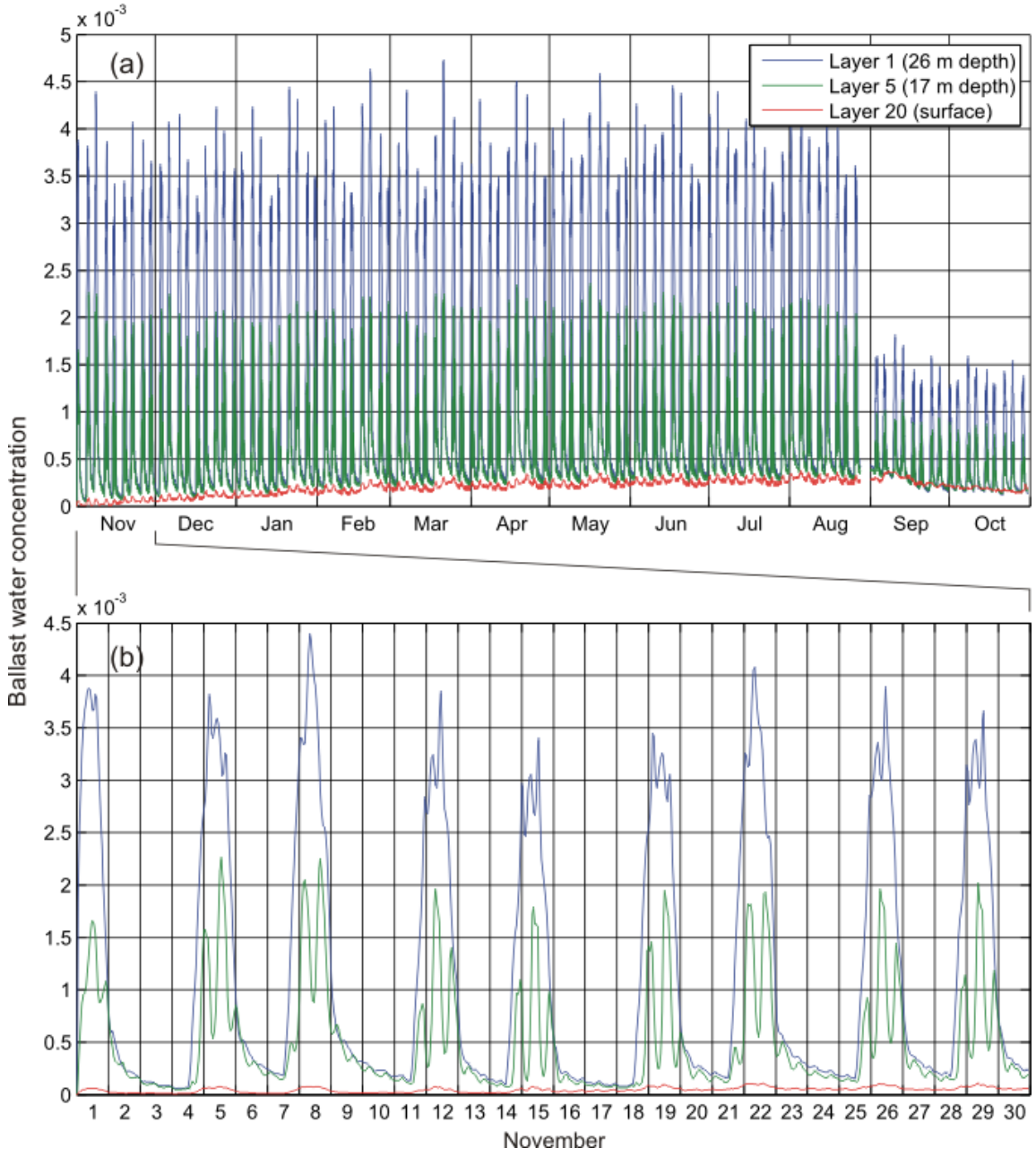

Figure 5. Example of the concentration records at Site 5 (near the ballast water discharge source). In the upper panel it can be seen that ballast water slowly accumulates in the system (as shown by surface concentrations; red line) during ice-covered conditions. Gradually reducing concentrations during the ice-free period (September-October) indicate that the ballast water is being flushed from Steensby Inlet..

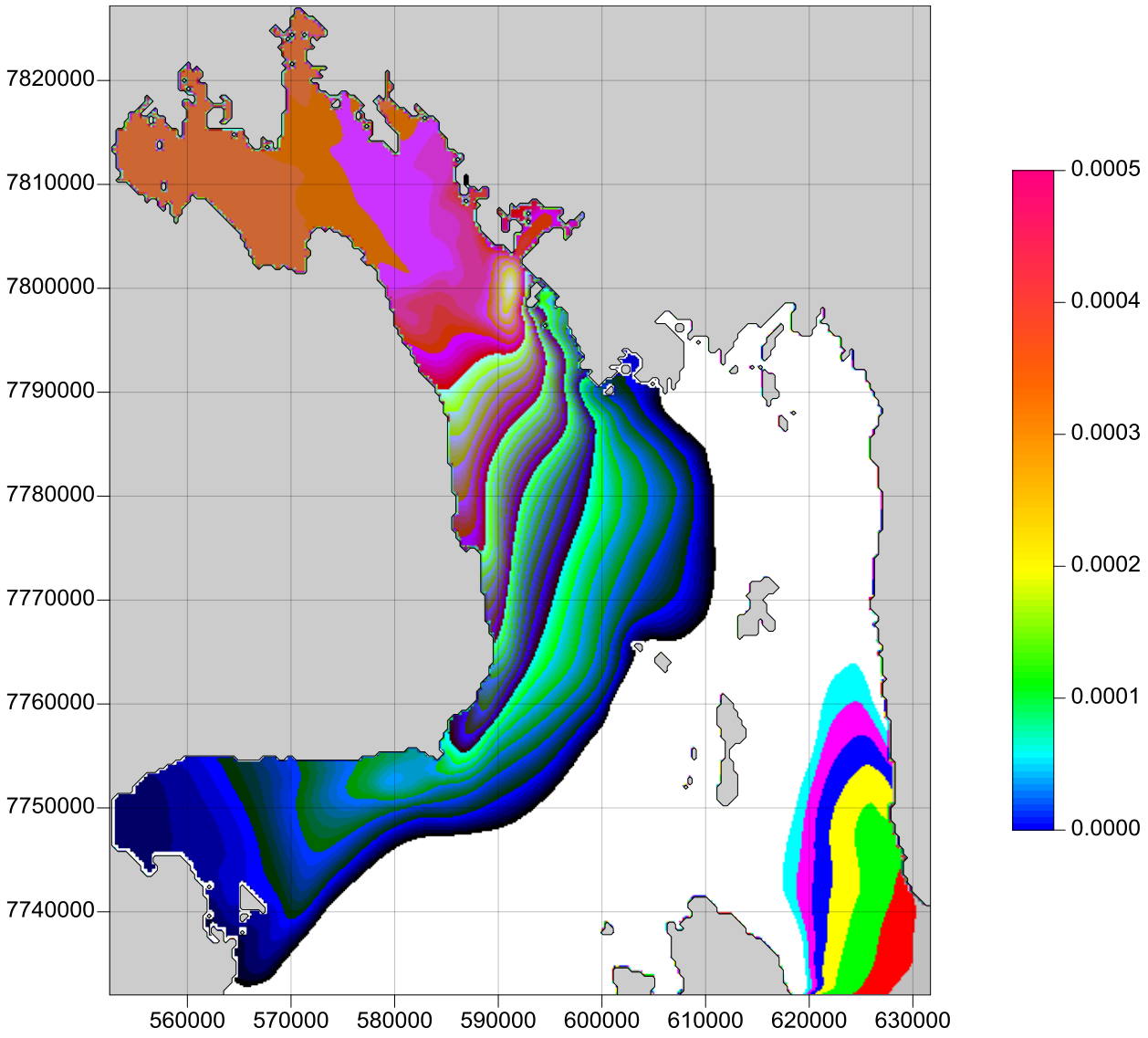

Figure 6a. Depth-averaged concentration of ballast water at the end of the ice-covered period.

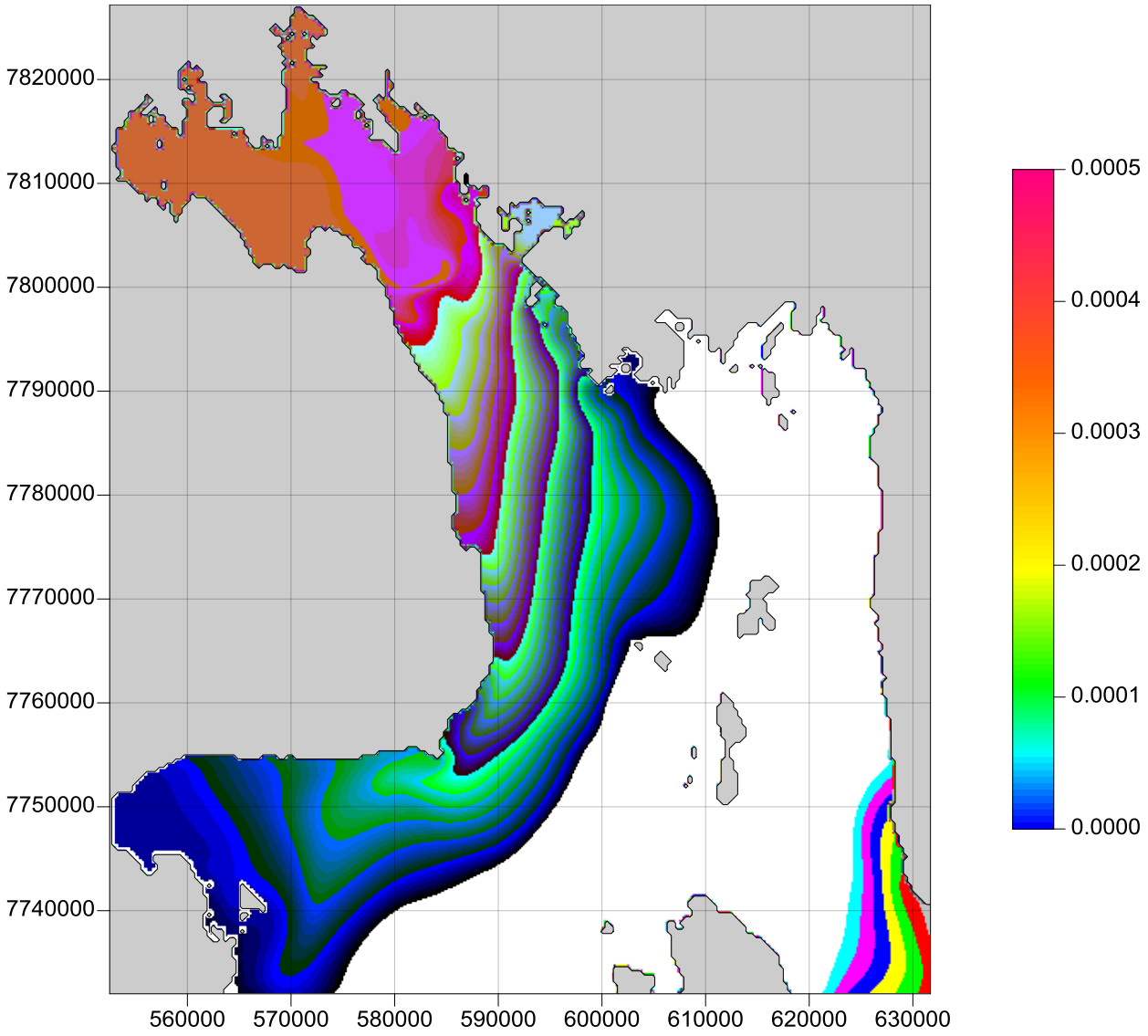

Figure 6b. Surface water concentration of ballast water at the end of the ice-covered period.

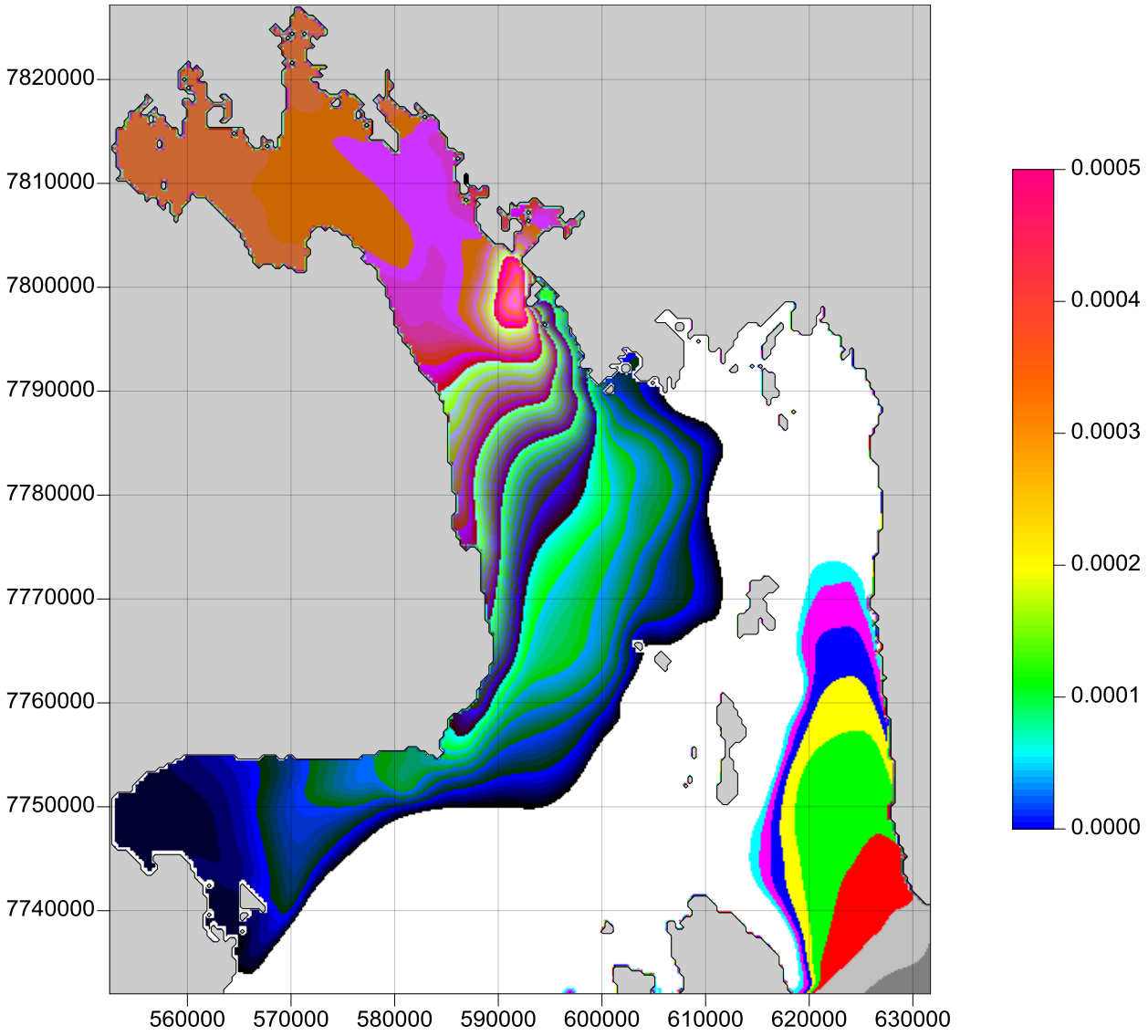

Figure 6c. Near-bottom concentration of the ballast water at the end of the ice-covered period

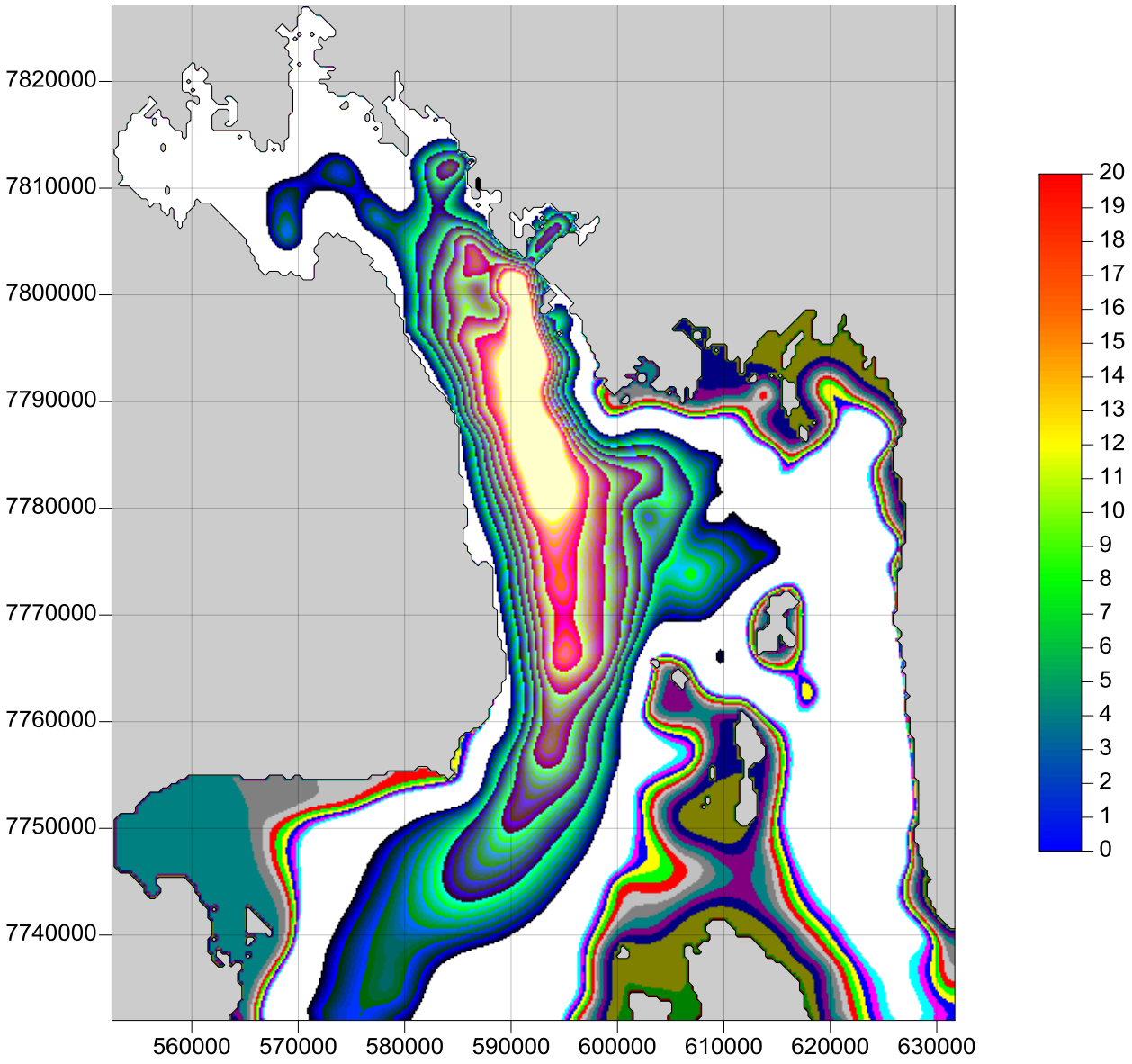

Figure 7. Depth-integrated contribution of ballast water (in mm) to the water column in Steensby Inlet at the end of the ice-covered period.

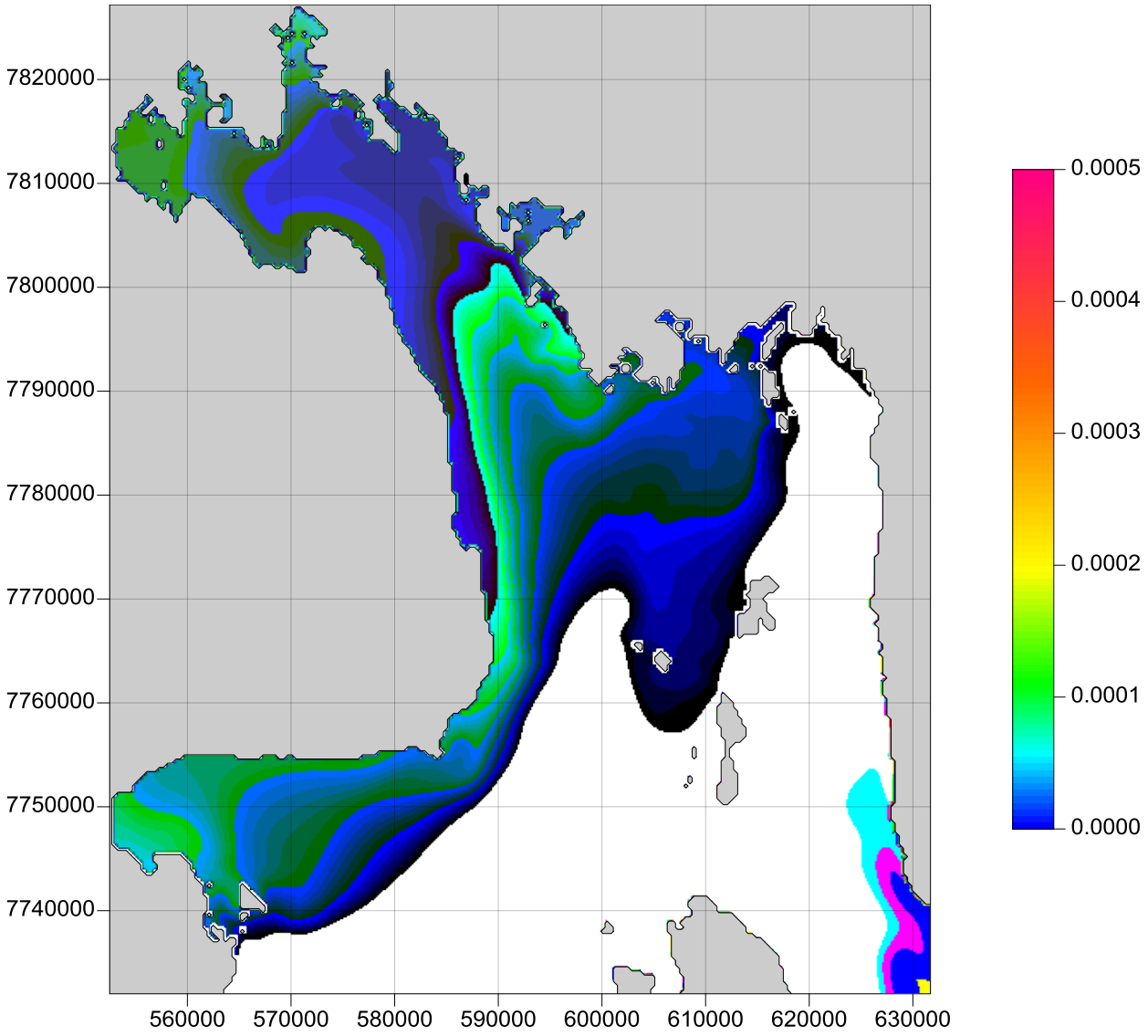

Figure 8a. Depth-averaged concentration of ballast water after 12 months (i.e., both ice-covered and ice-free periods).

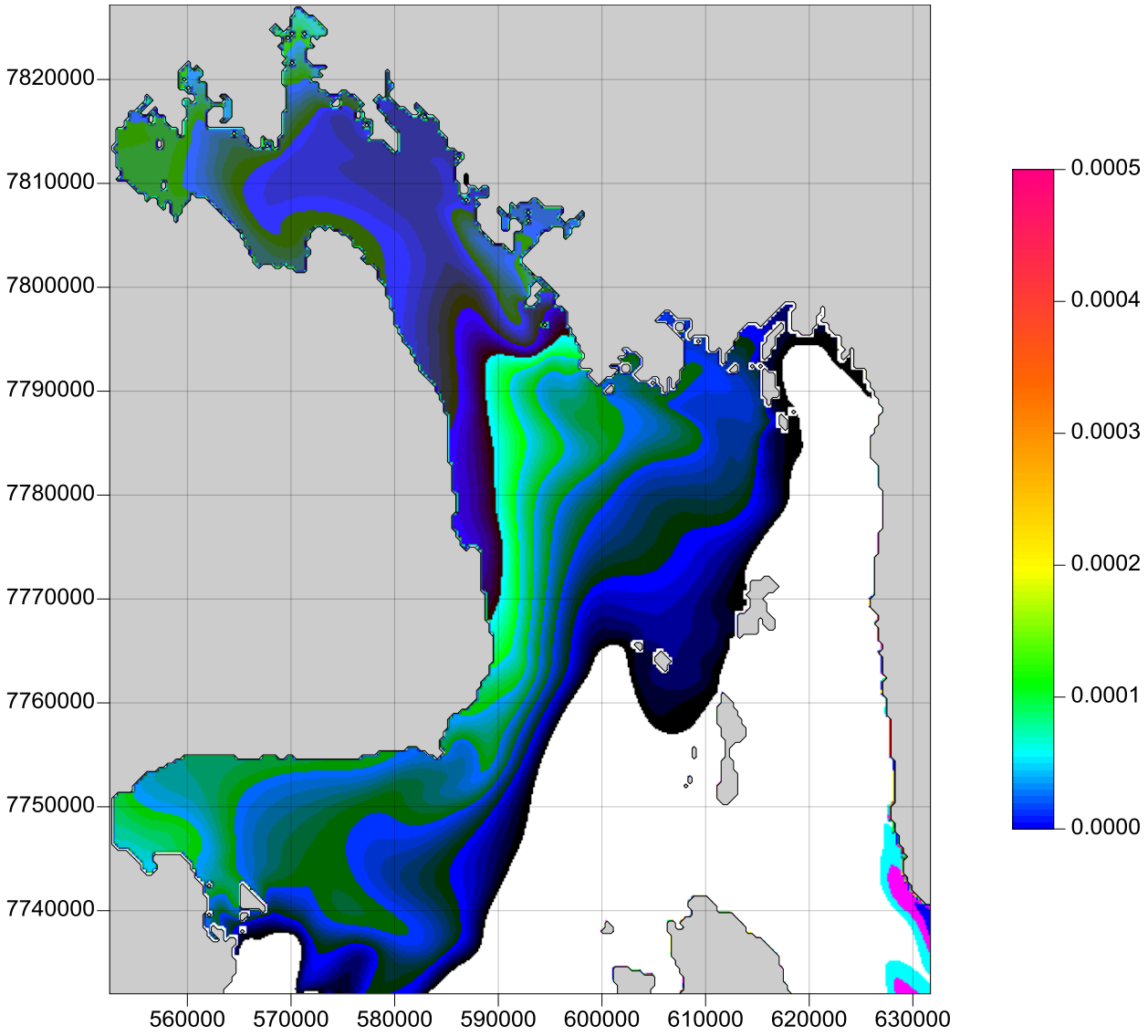

Figure 8b. Surface water concentration of ballast water after 12 months (i.e., both ice-covered and ice-free periods).

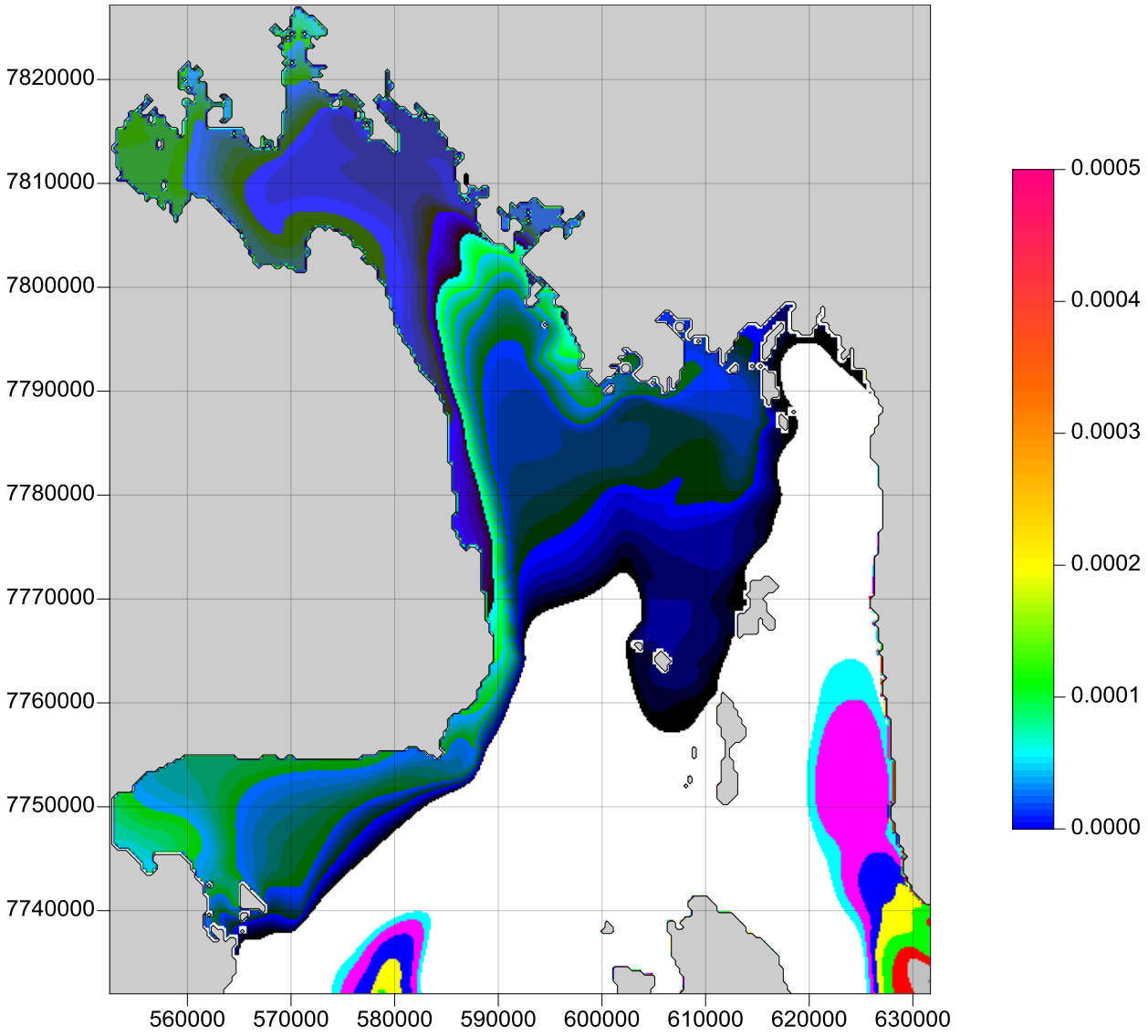

Figure 8c. Near-bottom concentration of ballast water after 12 months (i.e., both ice-covered and ice-free periods).

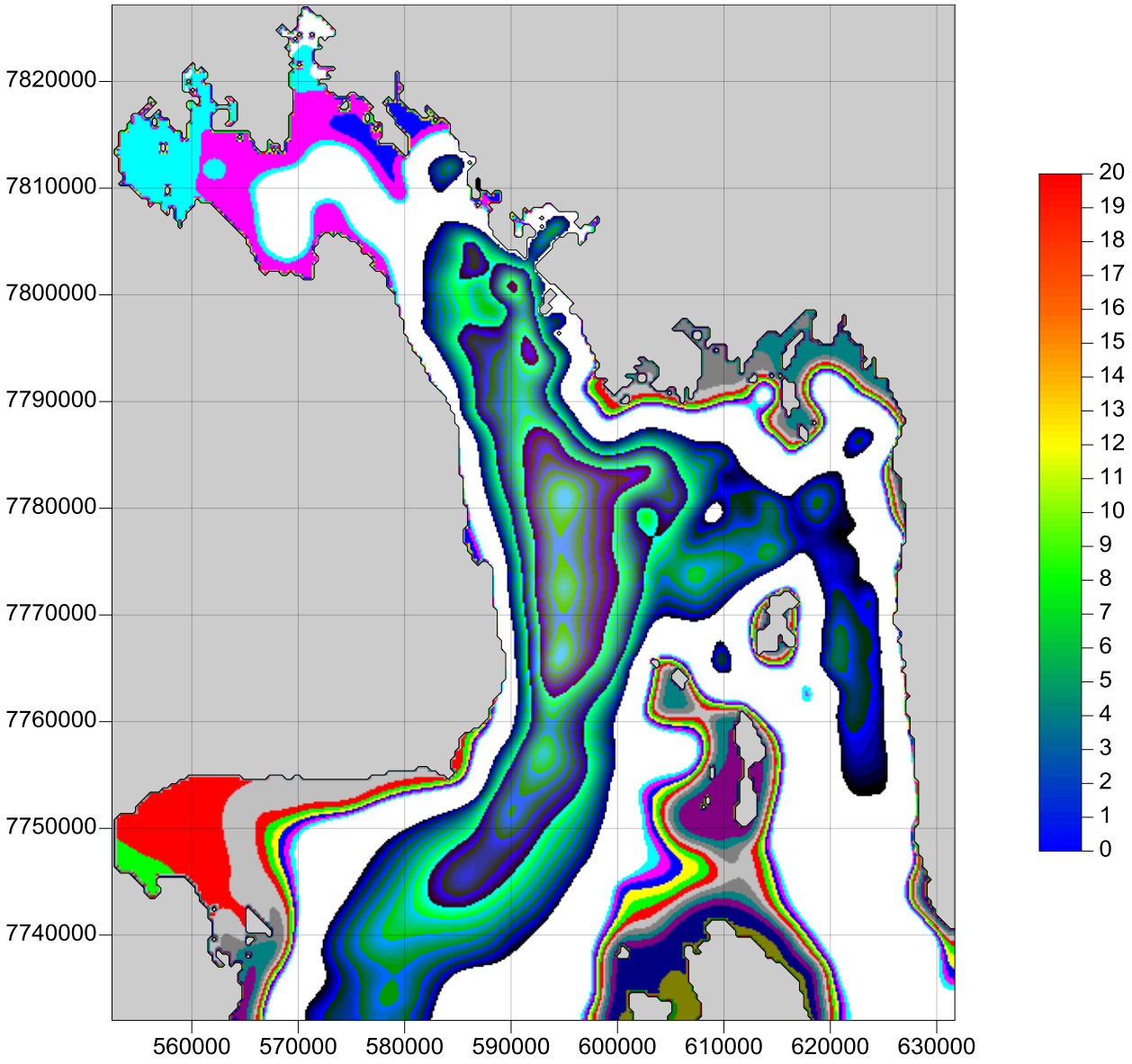

Figure 9. Depth-integrated contribution of ballast water (in mm) to the water column in Steensby Inlet after 12 months (i.e., both ice-covered and ice-free periods).

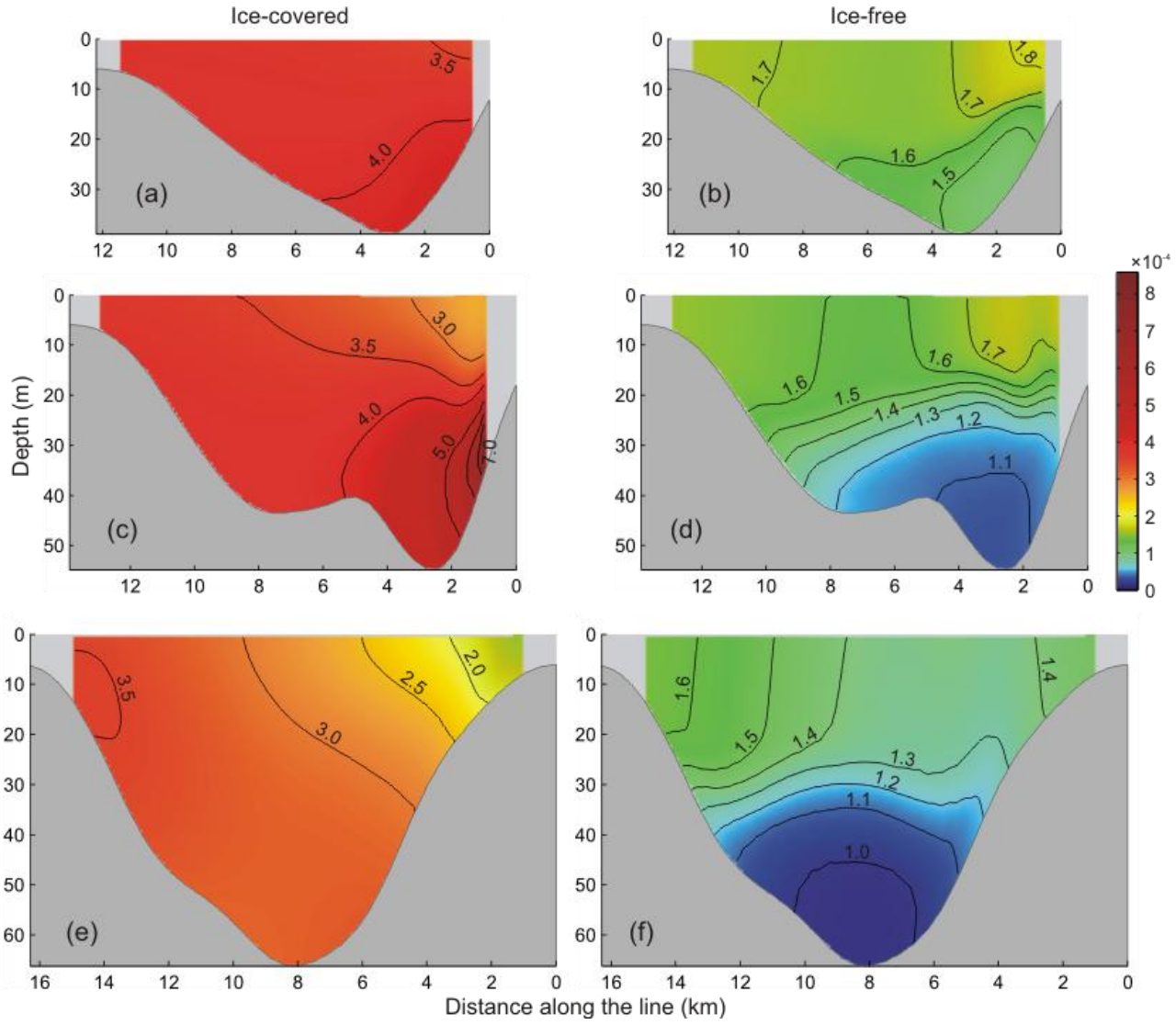

Figure 10. Vertical sections of ballast water concentration ($\times 10^{-4}$) at the end of the ice-covered period (panels on the left) and at the end of the ice-free period (panels on the right) along the red line (a, b), the blue line (c, d), and the green line (e, f). Cross-section positions are shown in Figure 2.

Sensitivity analysis

The results of the sensitivity analysis of ballast water dispersal, wherein discharge rates are doubled and halved, are presented in Figures11 through 14.

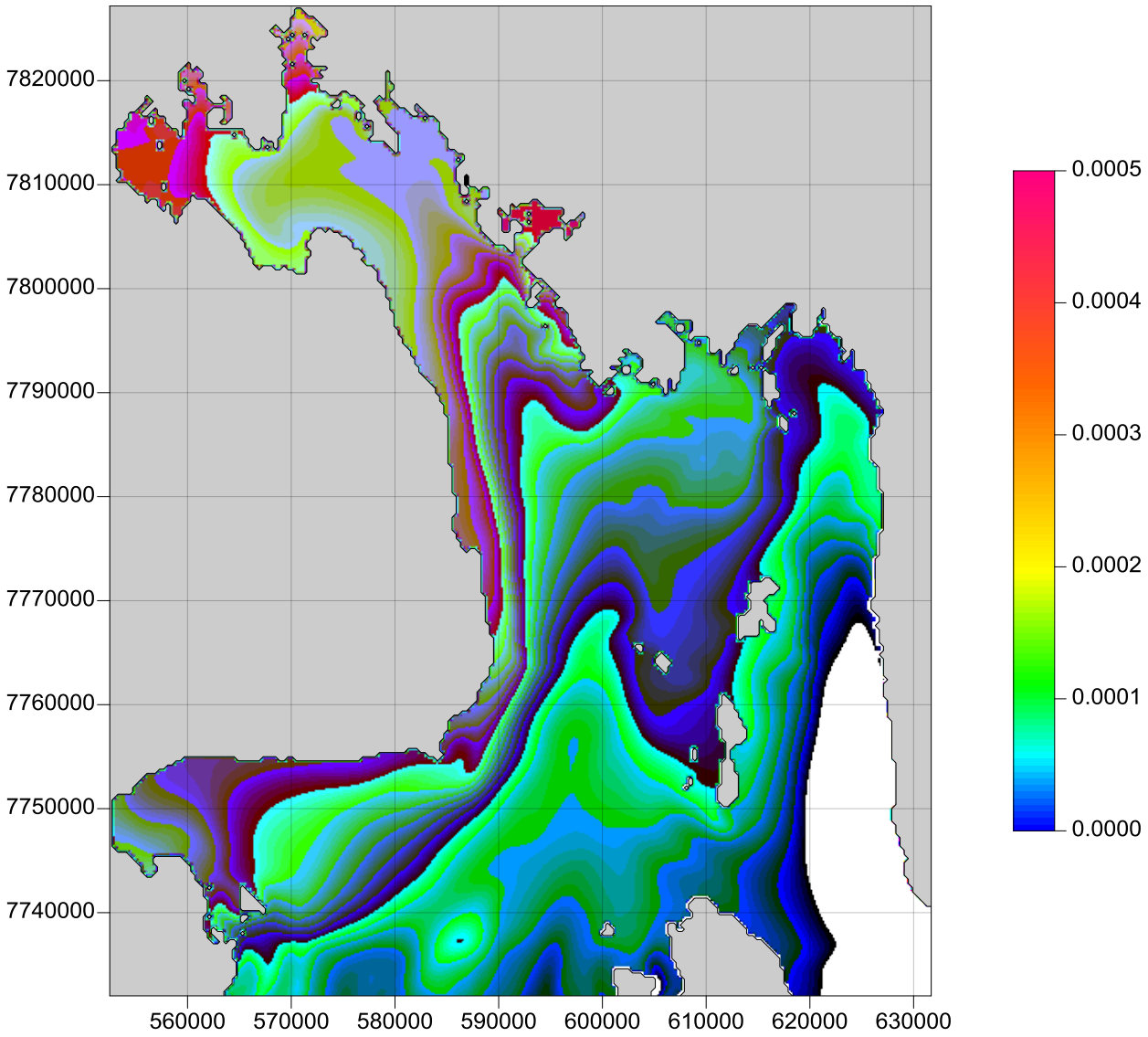

Figure 11. Depth-averaged concentration of ballast water after 12 months (i.e., both ice-covered and ice-free periods) with twice the ballast discharge rate.

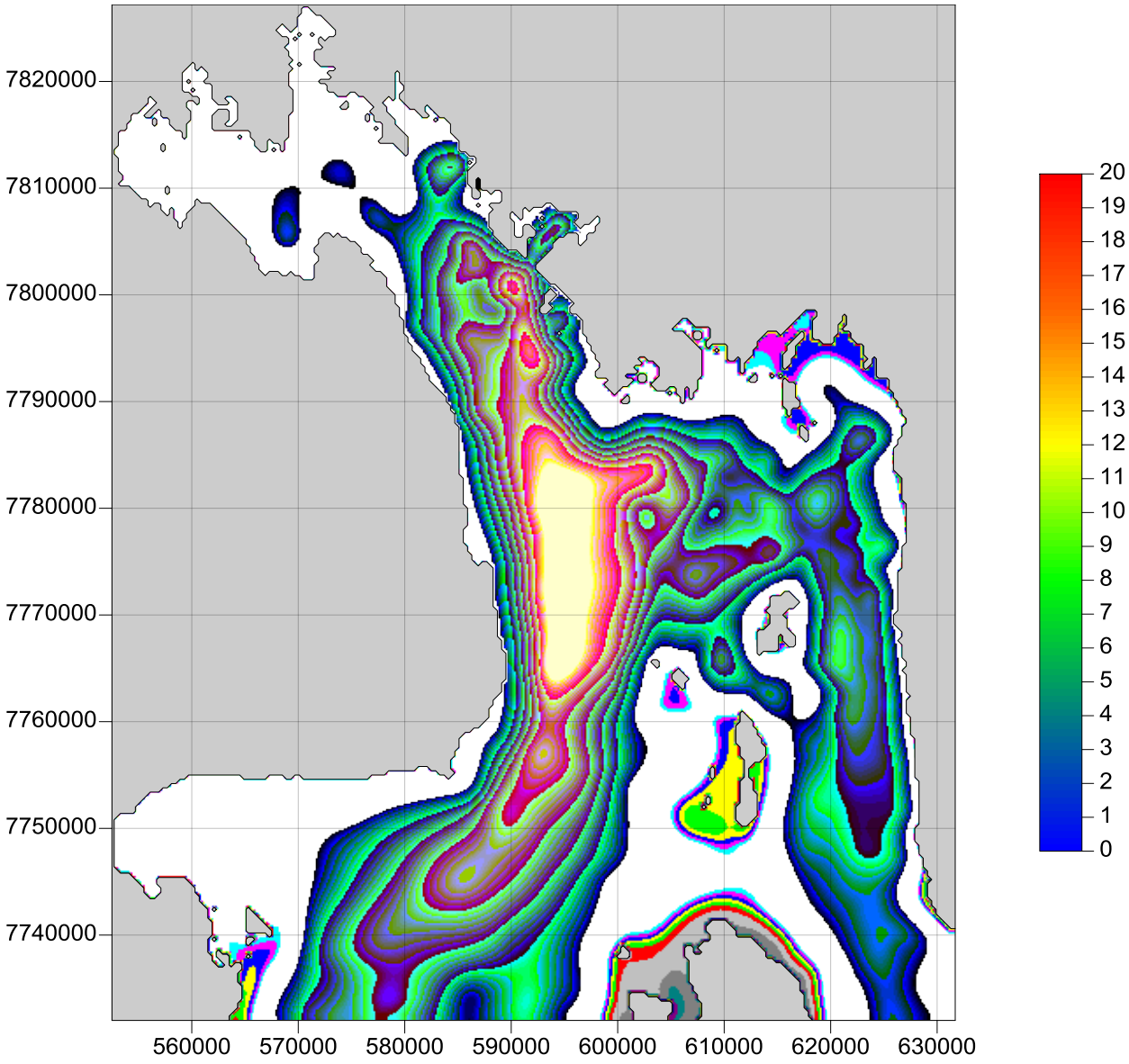

Figure 12. Depth-integrated contribution of ballast water to the water column (in mm) in Steensby Inlet after 12 months (i.e., both ice-covered and ice-free periods) with twice the ballast discharge rate.

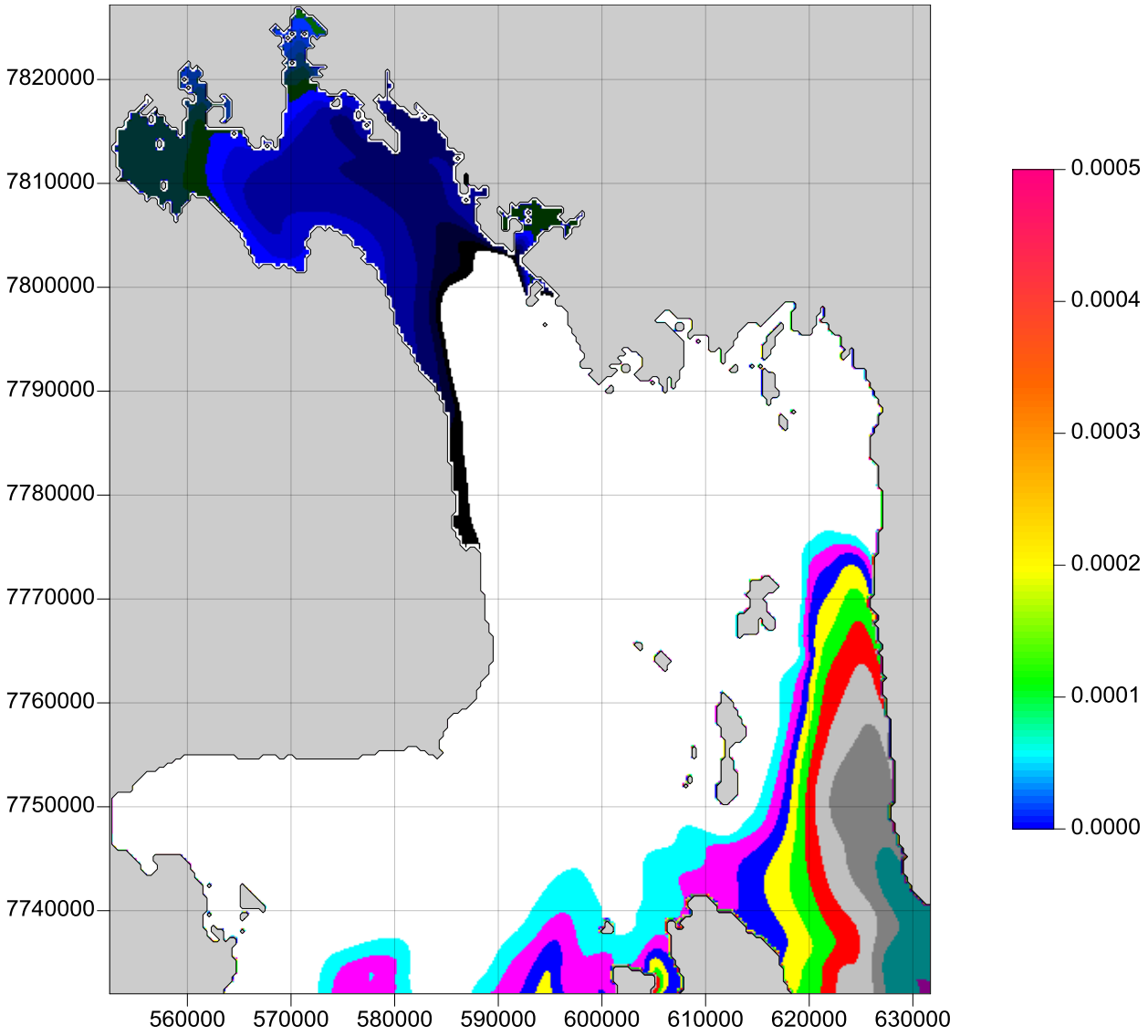

Figure 13. Depth-averaged concentration of ballast water after 12 months (i.e., both ice-covered and ice-free periods) for half the ballast water discharge rate.

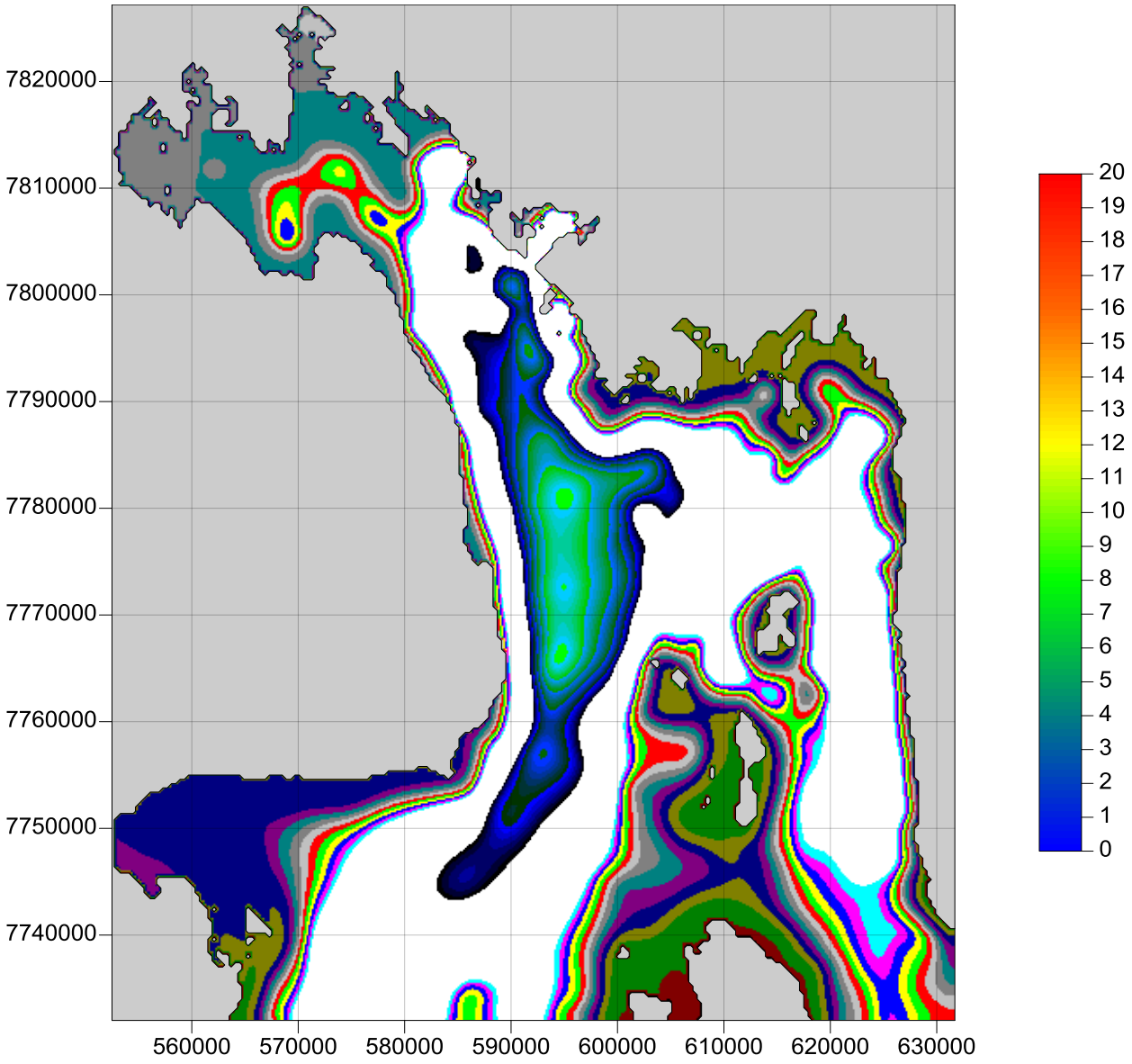

Figure 14. Depth-integrated contribution of ballast water (in mm) to the water column in Steensby Inlet after 12 months (i.e., both ice-covered and ice-free periods) for half the ballast water discharge rate.

Table 7. Summary of ballast water contribution to the Steensby Inlet system after 10 months of ice cover, and after 10 months of ice cover and 2 months of open water conditions

	Total water remaining to the north of the red line (Figure 2)		**Total water remaining to the south of the green line (Figure 2)**		**Total water remaining in the port area (between red and green lines; Figure 2)**		**Total water left the area through open boundary**		**Total released water**	
	10^6 m^3	**%**	**10^6 m^3**	**%**	**10^6 m^3**	**%**	**10^6 m^3**	**%**	**10^6 m^3**	**%**
After 10 months (end of ice-covered period)	1.53	8.9	11.55	67.3	2.46	14.4	1.60	9.4	17.15	100
After 12 months (end of ice-free period)	0.69	3.7	9.47	51.5	0.98	5.3	7.3	40.0	18.4	100

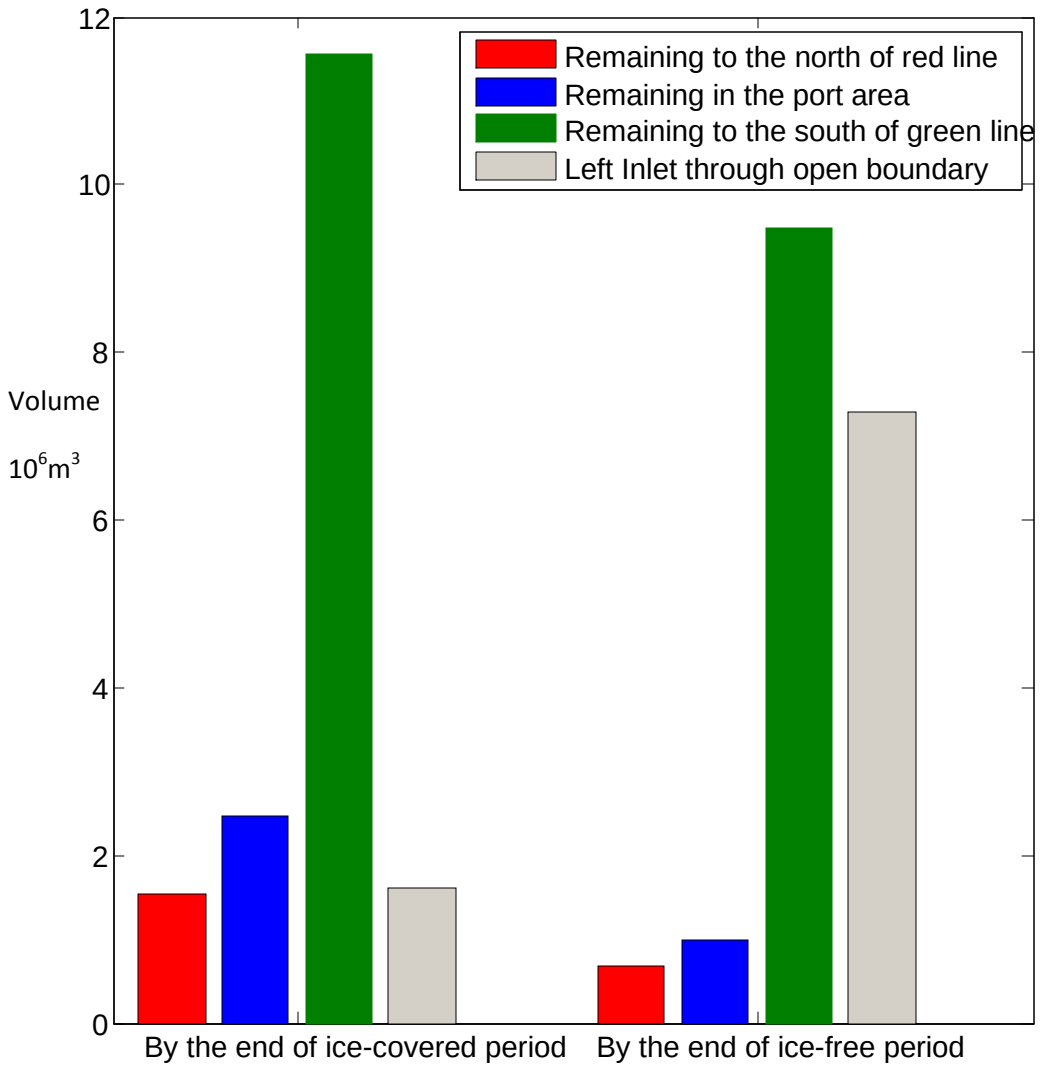

Figure 15. Ballast water budget by area (corresponding to Table 7) (See Figure 2 for locations).

Conclusions

A circulation model was developed for Steensby Inlet, forced by an existing large-scale circulation model for Foxe Basin, and validated using tidal, wind, ADCP and CTD data collected in Steensby Inlet. The model was in a very good agreement with the observations.

Using this circulation model, a coarse-grid, preliminary estimation of the ballast water dispersal pathways and concentrations, based on the application of the Regional Ocean Modeling System (ROMS) in Steensby Inlet after one year of discharge, revealed the following attributes:

1. Most of the ocean currents in Steensby Inlet are of tidal origin with strongly dominating semidiurnal currents. A weak counter-clockwise circulation regime exists in Steensby Inlet with new water entering the inlet in the southeast from Foxe Basin and exiting in the southwest.

2. In addition to the tides, both wind-induced and estuarine circulation is important during the ice-free period.

3. Ballast water, originating in the North Atlantic, is entrained in ambient seawater to be distributed throughout much of Steensby Inlet, particularly in the northern, western and south-western sectors, under both ice-covered and ice-free conditions. The south-western sector has the greatest depths in Steensby Inlet.

4. Advection is, as expected, more significant during ice-free conditions due in large part to a stronger estuarine circulation regime bringing in more bottom water from Foxe Basin and delivering a greater volume of southward-flowing fresher surface water.

5. After 10 months of ballast water discharge, under ice-covered conditions at the port site, ballast water concentrations within Steensby Inlet are seen to be still rising. Open water, wind-driven, and especially estuarine circulation, however, intensifies the advection, nearly clearing ballast water from the northern part of the Steensby Inlet system. Some ballast water remains in Steensby Inlet at the beginning of the next ice-covered season.

6. Ballast water concentrations are low everywhere, even when discharge rates are doubled. All values are below 0.05%. The concentration of ballast water at all places in the inlet varies nearly linearly with the discharge rate of ballast water.

7. Because of the greater water depths, the cumulative contribution of ballast water to the entire water column is greatest in the central and south-western parts of Steensby Inlet where values as high as 20 mm are found under the baseline conditions of 200,000 m^3

twice per week in ice-covered conditions and 70,000 m^3 twice per week during open water conditions.

More refined modelling can be undertaken using a fine-grid model near the port area, nested within the Steensby Inlet circulation model, to elucidate other processes such as gravity flows which might occur as ballast water is discharged at the port. Additionally, as new information becomes available on the vessel design and operations, these details could be incorporated into this next ballast water dispersion model.

References

AMEC Earth and Environmental, 2009, Steensby Inlet Oceanographic Monitoring – 2008 Data Report – Baffinland Iron Mines Corporation – Mary River Project. Report submitted to Knight-Piésold Ltd. By AMEC Earth and Environmental. January 2009. 189 pp.

ASL, 2008, BaffinLand Terminal Steensby Inlet – Sites "BLT1" and "BLT2" – Preliminary Current Results, May 2 to October, 2008.

RWDI, 2008, Baseline Meteorological Assessment, Baffinland Iron Mines Corporation Baffin Island, Nunavut. Report submitted to Knight-Piésold Ltd. by RWDI Air Inc. Project Number: #W07-5226A. Nov. 6, 2008. 141 pp.

SAUCIER, F.J., S. SENNEVILLE, S. PRINSENBERG, F. ROY, G. SMITH, P. GACHON, D. CAYA, R. LAPRISE, 2004. Modeling the sea ice-ocean seasonal cycle in Hudson Bay, Foxe Basin and Hudson Strait, Canada. Climate Dynamics, 23, Pages 303-326.

ST. LAURENT, P., F.J. SAUCIER, AND J.-F. DUMAIS, 2008, On the modification of tides in a seasonally ice-covered sea. Journal of Geophysical Research, 113, C11014, doi:10.1029/2007JC004614